Research Square

Preprints are preliminary reports that have not undergone peer review.
They should not be considered conclusive, used to inform clinical practice,
or referenced by the media as validated information.

Development of a Regional Landslide Forecast Model for Slowly Moving Landslides in the Western Canada Sedimentary Basin

Michael Porter
BGC Engineering
Corey Froese
corey@wavelengthadvisory.ca

University of Alberta
Caio Stringari
BGC Engineering
Vincenzo Coia
Politecnico di Milano

Method Article

Keywords:

Posted Date: July 27th, 2026

DOI: https://doi.org/10.21203/rs.3.rs-10168687/v1

License: This work is licensed under a Creative Commons Attribution 4.0 International License.
Read Full License

Additional Declarations: No competing interests reported.

Development of a Regional Landslide Forecast Model for Slowly Moving Landslides in the Western Canada Sedimentary Basin

Michael Porter[1], Corey Froese[2,3], Caio Stringari[1], Vincenzo Coia[4]

[1]BGC Engineering, Vancouver, BC, Canada

[2]Wavelength Advisory Services, Edmonton, AB, Canada*

[3]Department of Civil and Environmental Engineering, University of Alberta, Edmonton, AB, Canada

[4]Department of Civil and Environmental Engineering, Politecnico di Milano, Milan, Italy

*Corresponding Author; corey@wavelengthadvisory.ca; ORCID ID: 0009-0007-4805-172X

Abstract:

Large, deep-seated and slowly moving landslides encountered across the Western Canada Sedimentary Basin (WCSB) are crossed by all types of linear infrastructure and impact on populated areas on river valley slopes in the region. While these landslides do not lead to sudden or catastrophic loss they have historically lead to significant economic losses associated with mitigations caused by ongoing strain. While there is tolerance for movement built into the design of linear infrastructure crossing these landslides, there are maximum tolerances for the total amount of movement that can be accommodated before permanent damage occurs. If those movements occur quickly it reduces the opportunity for early identification and proactive mitigation. With this, infrastructure owners in the region contributed a large amount of regional displacement data (Froese et al, submitted) to support developing an understanding of spatial and temporal displacement trends over many decades. These displacement trends were then coupled with data on hydroclimatic drivers obtained from the ERA-5 Land global re-analysis model in order to better understand the specific components of wetting that correlated with increased landslide activity in order to identify key drivers that could be utilized to develop a warning model that could be calibrated with historical performance. This paper outlines how these various data were integrated, the development of the concept of a regional landslide activity index, the development of a forecast model and demonstration as to how the model performed as a hindcast when assessed against known events. The initial approach to utilize the model as a forward-looking forecast for the 2026 landslide season is also demonstrated.

1.0 Introduction

Across Western Canada, linear infrastructure such as pipelines are exposed to slowly moving deep seated landslides (DSL) where loading induces strain that impacts on the integrity and serviceability of these assets. A review by Porter et al (2019) indicated that it is estimated that at least $ 400 million per year is spent by asset owners to mitigate the impacts of landslide damage within this region. Part of the approach to managing the risks to these assets is determining the allowable strains and planning mitigation proactively to minimize economic impacts or environmental damage. Following significant regional accelerations of DSLs in the spring of 2020 throughout much of northern British Columbia and Alberta, Canada, a joint industry project was initiated to better understand the drivers for landslide activity change to support pro-active awareness in the future. This paper summarizes the development of the regional landslide forecast model that was supported by this research collaboration.

2.0 Regional Landslide Understanding

The Western Canada Sedimentary Basin (WCSB) underlies the prairie region of western Canada and is underlain by a deep sequence of sedimentary bedrock that has been shaped over time by multiple glaciations. The modern-day river valleys have downcut into thick sequences of glacial sediments and weak bedrock, leading to initiation of large valley slope failures over time (Figure 1). These initial failures have led to thick deposits of clay-rich colluvial soils that blanket valley walls.

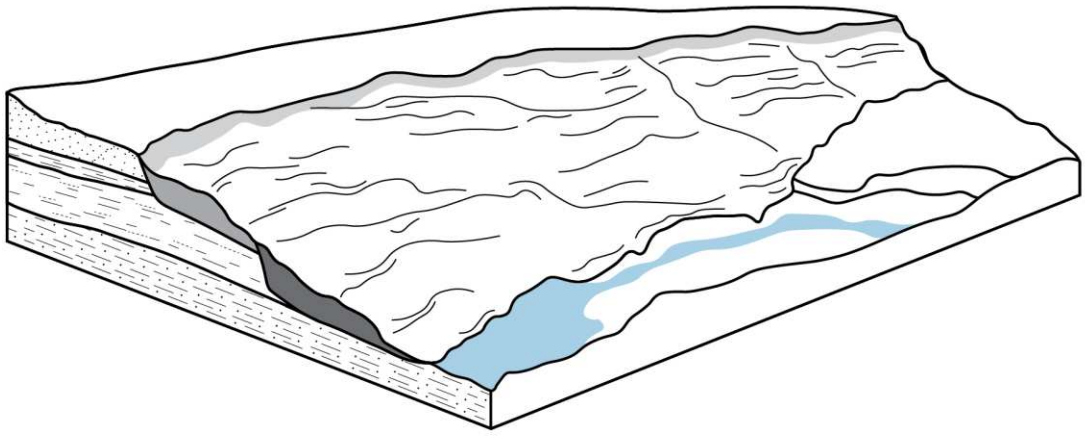


Figure 1. Idealized slope schematic providing a representation of the source zones and depositional patterns for deep seated landslides origination from both glacial soils and shale bedrock along modern watercourses across the study area.

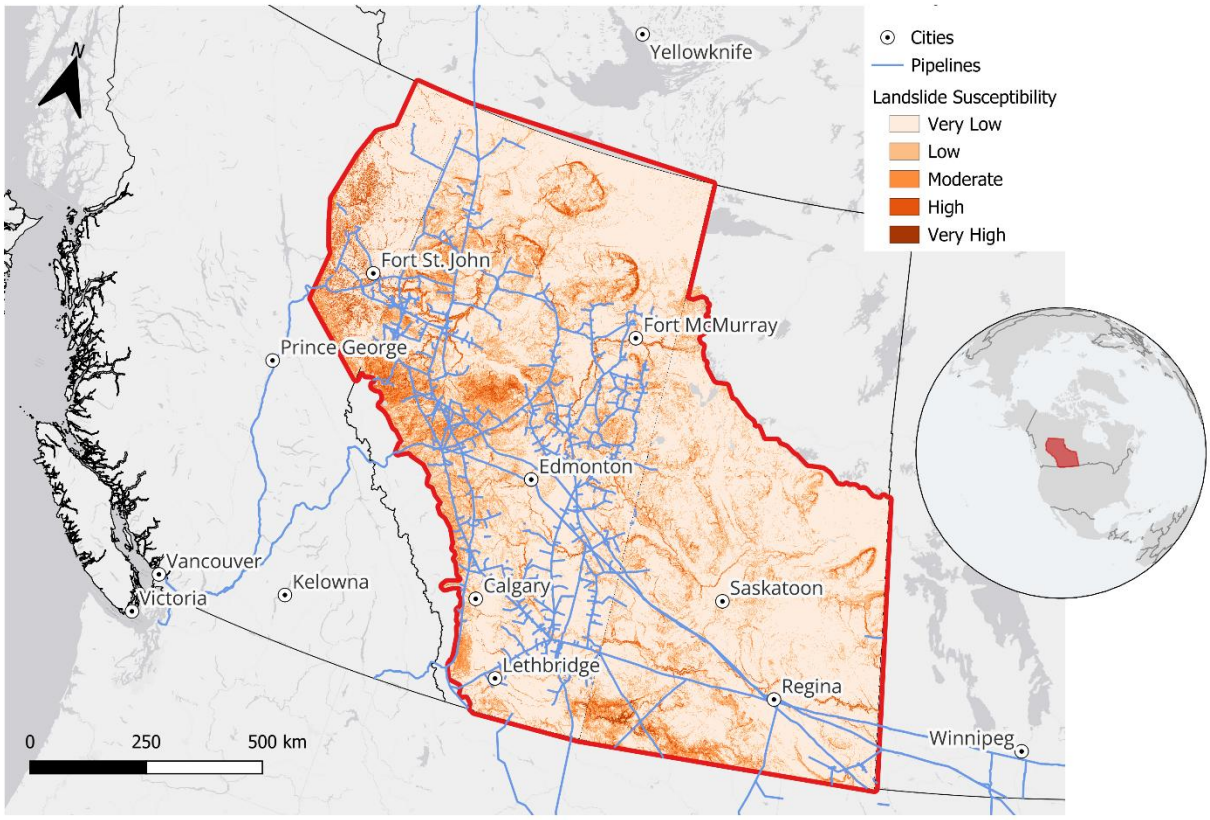


Figure 2. Regional landslide susceptibility model derived from BGC (2021), Pawley et al (2022) and Dowling et al (2019). Data Sources: ESRI tiles, Natural Earth and HIFLD (Homeland Infrastructure Foundation-Level Data) Canadian pipeline dataset.

Figure 2 provides an overview of the spatial landslide susceptibility across the WSCB that predominantly corresponds to the locations of these modern-day river valleys.

3.0 Understanding Operational Needs for Landslide Early Warning

The primary requirement of a landslide early warning system (LEWS) is to provide information on trends with sufficient lead time to take action to minimize the consequences of an increase in slope activity. For more localized and rapid slope processes the action may be focused on the closure of a specific asset or impacted element, while for a more regional system focused on DSLs, warning will typically influence the frequency of monitoring and inspection activities. Figure 3 provides a visual representation of the variability in both space and time that are considered in the design of a LEWS.

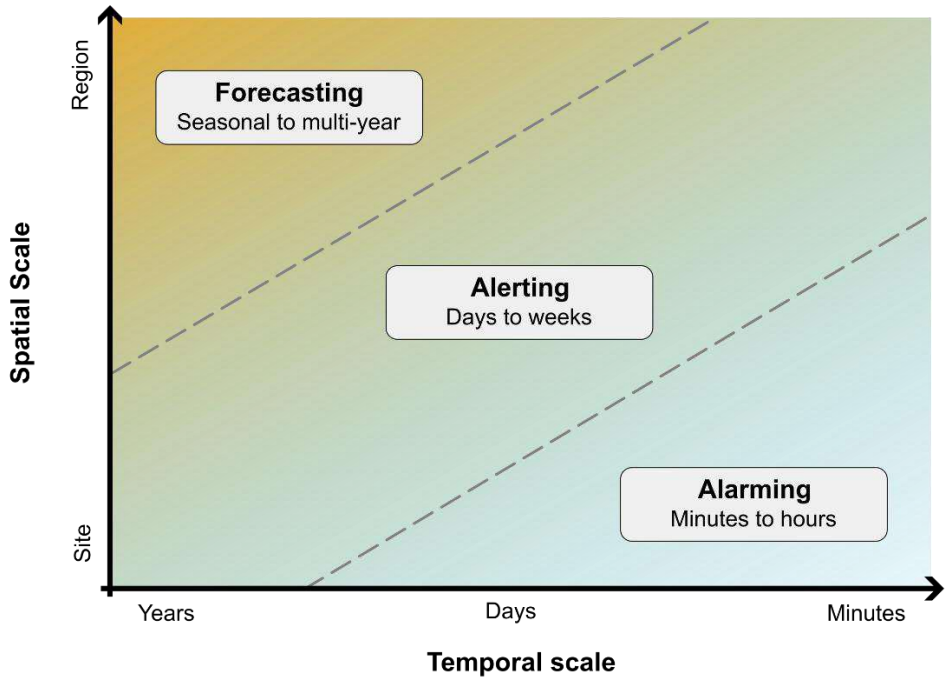


Figure 3. Schematic relating the resolution of warning required over different temporal and spatial decision-making frames

The terminology adapted on Figure 3 follows that utilized by Sattele et al (2016) which provides the following guidance around the timing of warnings with respect to response actions:

- Forecasting: for regional landslide processes, the scale at which the relationships between external drivers and landslide activity are defined in terms of the likelihood of populations of landslides becoming more active. Sattele et al (2016) describe these systems as having the lowest degree of automation as trend data is reviewed at regularly schedule intervals and incorporated into forecast bulletins generated by subject matter experts. This knowledge is used by different types of asset managers to triage different types of responses. For shallower landslides, this awareness is likely a seasonal understanding of the likelihood of increasing landslide activity. For deeper seated landslides, with increased importance of longer (multi-year) moisture infiltration, awareness requires a multi-year (to decade) understanding of trends and the ability to understand how seasonal inputs overlay on the broader trends.

- Warning: this type of LEWS can be applied at both the regional and local scale and is based on the ability to be able to define the variables that are expected to precede an intolerable displacement. Sattele et al (2016) define these systems as being at least partially automated and design to monitor the precursors to a slope collapse over an extended time frame. Typically, the trends are routinely reviewed against thresholds that trigger review and actions, such as evacuations,

by decision makers. At the local scale, the parameter that is measured may be the direct displacement of the landslide (surface or subsurface). At a regional scale this may involve setting thresholds for hydroclimatic parameters that have been correlated to landslide activity changes. Regardless, this level of LEWS is based on the premise that there will be a progression of alerts that will escalate prior to a collapse such that appropriate preparedness activities can be undertaken.

- Alarming: Sattele et al (2016) described these systems as being fully automated, designed to detect ongoing process parameters with short lead times and to measure against thresholds that serve as a decision instance. This is typically defined as the detection of a rapid event immediately after failure such is applied for processes such as rockfalls, debris flows and avalanches. These type of LEWS are typically focused on local processes and designed to provide warning that will minimize exposure of populations to the landslide. These types of systems can be utilized to close linear transportation routes such that people and vehicles are not exposed to an event. These systems would be comprised of local measurement sensors with on-site power and telemetry that is used to relay messages to decision makers. In some cases, data loggers are programmed with decision logic such that actions, such as road closures, are automated.

For DSLs, infrastructure located on or within these features is typically designed to allow for a certain amount of strain (Mansour et al, 2011) and techniques such as Finite Element Analysis (FEA) modelling (Conte et al, 2014; Sengani et al, 2022) are utilized to determine the allowable strain prior to the requirement for mitigation. For pipelines, these strains are measured (Dewar et al, 2016) and the range of actions that may be considered to mitigate against an intolerable accumulation of strain may include measures to stabilize the slope, measures to relieve strain on the pipeline, or replacement of the pipeline to a location that is less impacted by the strain (directionally drilling under a landslide or moving to a more stable location) (Ahmadipur et al, 2020). As there is often a significant cost to any mitigative measure and likely many potential mitigation sites, asset managers are often juggling competing demands for limited resources. To determine when and where to most effectively deploy resources, asset managers must understand which landslide hazards create the largest risk to determine where to act and information as to when landslides are expected to be more active to determine optimal timing for mitigation (Porter et al, 2023).

When considering the ability to track the activity and velocity of DSLs at the regional level, it is not reasonable to expect that all slopes will perform uniformly. In part, this is because changes in soil moisture and porewater pressure are just one of many factors controlling slope stability, and even these factors will not change uniformly across a region. In any given year, some landslides are likely to increase in velocity while others are likely to slow

down. Therefore, attempts to assign a likelihood to the proportion of slopes in a region that may experience an increase or decrease in activity and velocity are more likely to be successful. For example, when considering shallow landslides in the Pacific Northwest region in the United States, Mirus et al (2018) utilized linked antecedent soil moisture and a short duration precipitation accumulation to develop a simple classification system that described the likelihood of regional landslide accelerations as Unlikely, Possible and Probable in the regional context.

Similarly, when considering the linkages between hydroclimate variables and DSLs in a regional context in the Emilia Romagna region of Italy, Segoni et al, (2018) provide perhaps the most comprehensive attempt to link regional trends in landslide activity to hydroclimatic drivers. This region was divided into a series of Alert Zones where over two decades of slope displacements were recorded and coupled with data obtained from regional rain gauges to establish relations between longer duration soil wetting from precipitation and shorter duration events to define alert levels. These alert levels were communicated as the likely number of landslides to accelerate within each Alert Zone and were defined as absent (0 to 1 landslide), low (2-19 landslides, moderate (25 to 59 landslides) and high (more than 60 landslides).

For the WCSB, the objective is to understand how populations of landslide are expected to react in response to hydroclimatic forcings. Therefore, the objective of an early warning model and system is to provide awareness across an operational region to understand how trends are developing and can be integrated into decision-making. As operational budgets are often determined over multi-year time frames, the understanding of trend development over similar time frames is required to be of value. Accordingly, our landslide and warning model development focuses on analysing annual displacement trends to quantify their relative rarity and recurrence as a foundation for forecasting future activity.

4.0 Understanding Relationships Between Broad Hydroclimatic Trends and Activity for Slowly Moving Landslides

4.1 International Experience

While there has been significant documentation of the development of warning and forecasting services for rapid and shallow landslides based on precipitation thresholds, as reviewed by Guzzetti et al (2020), there have been less well documented examples for forecast systems for DSLs at the regional scale. When considering DSLs many researchers have identified the key role of subsurface water balance (Zieger et al, 2023; Handwerger et al, 2013; Finnegan et al, 2021) and the need to characterize the linkages between broader hydroclimatic inputs and landslide activity (Coe et al, 2012; Lacroix et al, 2020). Others

have also utilized instrumented sites to support the understanding of the importance of characterizing the longer-term antecedent conditions in conjunction with transient precipitation to support improvement of landslide early warning models (Wicki et al 2021). Recently, Rana et al (2026) utilized Persistent Scatterer Interferometric Aperture Radar (PS-InSAR) techniques applied to X-Band SAR data to characterize key inflections in displacement trends and have utilized a hydroclimatic variable termed the Antecedent Precipitation Index (API) to support characterization of the soil moisture trends that correspond with these displacement deflections and have demonstrated the utility of this methodology around a key measurable event from 2015.

For regions where there are not extensive longer term hydroclimatic monitoring stations corresponding with landslide locations, there has been more reliance on the use of global hydroclimatic models that utilize both modelled precipitation and soil moisture to support development to LEWS models (Distefano et al, 2023; Handwerger et al, 2013; Khan et al, 2022). These studies have demonstrated the improvement in model performance by integrating soil moisture rather than solely precipitation data. Similarly, in designing the LEWS for the Emilia Romagna region in Italy, Segoni et al (2018) demonstrated how the incorporation of snow accumulation and melting, coupled with antecedent wetting from precipitations improved forecasts.

This current study focuses on how the historical measured displacement data trends across a regional network of instrumented landslides were evaluated in relation to long duration precipitation and soil moisture trends obtained from the ERA-5 Land Re-analysis product to support the development of a forecast model for DSL activity in the study region.

4.2 Relating Soil Moisture to Landslide Activity in the WCSB

During the initiation of the study of the drivers of DSLs in the WCSB, a review of available sources regional modelled datasets that could provide both spatial and temporal continuity across the region were explored (Froese et al, submitted). As there were historical displacement data and experience of the project team back to the early 1990s, the overall focus of the review was to find a modelled soil moisture product that provided the longest time history to allow to review against the displacement dataset. In reviewing the application and experience in the literature in evaluating available datasets (Zandler et al, 2020; Li et al, 2025; Alaminie, 2024) the ERA-5 Land Reanalysis model from the European Centre for Medium Range Weather Forecasts (ECMWF) (Munoz Sabater et al., 2021; ECMWF, 2016) was selected for initial exploration due to its suitability for evaluating long-term trends and characterizing normalized soil moisture relationships.

4.2.1 ERA-5 Land Re-Analysis Soil Moisture Data

ERA-5 Land (ERA-5) is a climatological re-analysis data product produced by Copernicus Climate Change Service (C3S) of the European Union (EU) and administered by the European Centre for Medium-Range Weather Forecasts (ECMWF). The reanalysis model spans 1950 to present on a 11 km horizontal grid at an hourly time step (Muñoz Sabater et al., 2021). ERA-5 is a global numerical model which couples the atmospheric, land, and ocean models (Munoz Sabater et al., 2021). Observations are assimilated from direct surface, ground, air, and water measurements, and from indirect satellite observations (Munoz Sabater et al., 2021; ECMWF, 2016).

ERA-5 data was accessed via Google Earth Engine (Muñoz Sabater et al., 2021) where the multi-variable hydroclimatic history, from 1950 to present, for any location in the world can be rapidly extracted and visualized. This provides the option for scalability and decadal analysis of the hydroclimatic conditions for any slopes located within 11 km grid cells. It is important to point out that the application of a common set of hydroclimatic conditions to this size of cell would not be able to reflect different landslide activity attributes that are impacted by local topographic or micro-climatic effects when assessing relationships at any specific slope. Therefore, it is important to understand that this modelled data is not expected to replicate the conditions at any landslide but to provide reliable trends to support the understanding of the changing conditions over time across a sub-region.

ERA-5 models volumetric soil moisture using a four-layer soil at the following depths:

- Layer 1: 0 – 7 cm
- Layer 2: 7 – 28 cm
- Layer 3: 28 – 100 cm
- Layer 4: 100 – 289 cm.

The bottom boundary condition assumes free drainage, which is a potentially problematic assumption for association with ground movements driven by pore-pressure increases as typically these soil/bedrock types are not free draining and do not readily dissipate pore pressures over short time periods. However, so long as this limitation is recognized, the soil moisture model provides a valuable indication of the deeper groundwater recharge conditions over time, particularly at a relative scale (ECMWF, 2016).

4.2.2 Assessing qualitative linkages with landslide activity

Engineers working in the WCSB over the past 35 years indicated that there have been specific “bad landslide years” where landslide accelerations have led to either damage of infrastructure or requirements for emergency mitigations. Based on this feedback, a set of key sites with well documented histories of accelerations and mitigations was compiled to support the initial qualitative evaluation as to the relations between these events and the historical hydroclimatic data obtained from the ERA-5 model. Information on the regional location of these sites and the key periods of elevated activity are provided in Table 1.

Table 1. Key sites with well documented elevated activity periods triggering an operational response.

Area	**Site ID**	**Periods of Elevated Activity Triggering an Operational Response**
Northeastern British Columbia	A	March 2017 to November 2021
	B	September 2018 and June 2020
East-Central Alberta	C	September 2011 to May 2015; June 2019 to March 2021
	D	March 1996 to May 1998; March 2001 to May 2002
Northeastern Alberta	E	March to August 2013; March 18 to February 2019; March 2020 to November 2021
	F	June 2012 to August 2013; June to August 2014; March to August 2020
	G	March 1997 to May 1998; March 2013 to February 2014; March to August 2020; March to May 2021.

As shown on Table 1, over the period from the late 1990’s to present there were specific periods across northern Alberta and British Columbia where periods of elevated activity were observed. To better understand the drivers of these elevated periods of activity, the Layer 4 Volumetric Soil Moisture (m^3/m^3) was first utilized to assess whether soil moisture trends appeared to qualitatively correlate with landslide activity. Initially, the reported Layer 4 values obtained from the ERA-5 model were utilized, without normalization, to assess how modelled trends correlated with measured landslide activity. Figure 4 provides an example for Site G listed in Table 1 where the displacement data collected

were plotted in relation to hydroclimatic variables anomalies (Layer 4 Volumetric Soil Moisture, Snow Melt and Precipitation) to assess initial qualitative relationships.

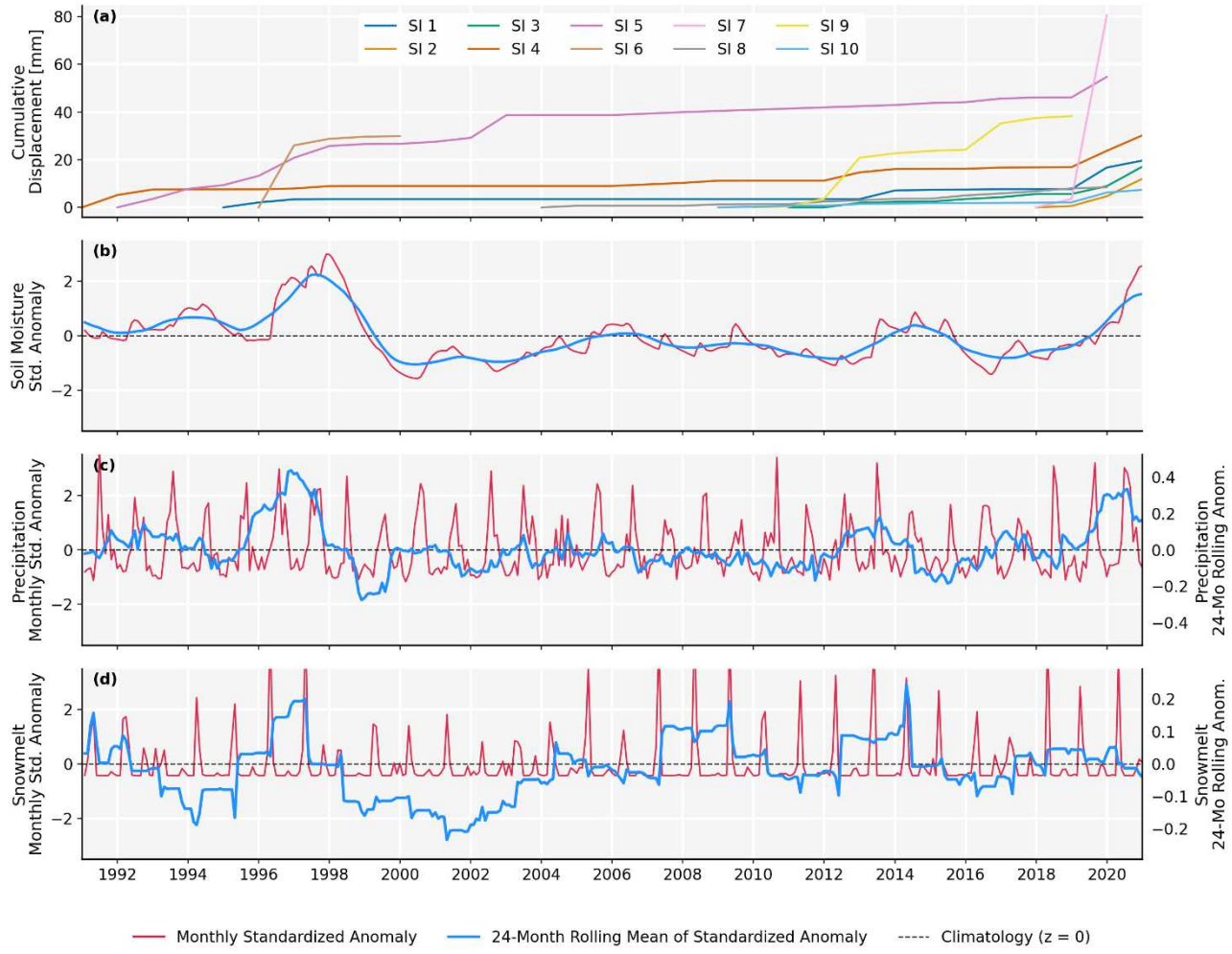


Figure 4. Example of a) SI cumulative displacement timeseries, b) volumetric soil moisture, c) precipitation and d) snowmelt anomaly timeseries for Site G.

The key observation from these visualizations was that periods of elevated modeled volumetric soil moisture generally coincided with intervals of increased displacement measured by slope inclinometers or inferred where casing shear prevented continued readings. These initial relations supported the team in further considering these qualitative relationships to provide a more rigorous quantitative relationship between hydroclimatic parameters and landslide activity. A more in-depth discussion of the ERA-5 model parameters and incorporation into the landslide and warning models are described in Section 4.2.1.

4.0 Landslide Model Data Inputs

Calvello (2017) has described the key components and considerations required for the design of a LEWS for weather-induced landslides as follows:

- Landslide Model: this component focusses on developing a model that supports the understanding of the linkages between landslide displacements and external drivers. Calvello (2017) defines this as "a functional relationship between weather characteristics and landslide events considering monitoring data and the geological, geomorphological, hydrogeological and geotechnical features of the area of interest". For the WCSB this involves determining the type of landslide activity for which the model is being developed, developing a spatial and temporal picture of the variability in the landslide activity (Froese et al, in preparation) and acquiring complimentary activity on the hydroclimate over space and time to support developing a predictive model.
- Warning Model: a warning model utilizes the relationships developed in the landslide model and considers the end-user needs and capabilities in order to determine as to which trends to track and how this knowledge would be utilized to support operational decisions. As discussed above, the context around why warnings are required, what are the response capabilities and how the information derived from the LEWS will be utilized by the decision maker drive what type of model is developed. From this understanding, the type of data considered and determination of appropriate alert and response actions will be considered. As an example, if considered as part of a forecasting system, a model may be utilized to forecast the likelihood of a change in activity in the population of landslides in region, while for an alarm system, thresholds may be set to correspond to different shorter term response actions such as road closures or evacuations.
- Warning System: Calvello (2017) outlines the key sub-components of the warning system as the warning dissemination, communication and education, community involvement and the emergency plan. Although the progression through landslide model to the warning system appear to progress in a linear system, the "human" components of the warning system drive the requirements for both the warning model and the approach to dissemination. The dissemination is the key technology component of the warning system that involves data management, connectivity and consideration for how and when alerts are delivered to the key decision makers in a timely manner.

The primary objective of outlining these components is to demonstrate the linkages and dependencies between the three components in supporting an operational LEWS. The initial discussion will focus on how the regional dataset required to support the development of the landslide model was developed and how decisions were made as to which data on which to focus and more reliably be integrated into the model development.

4.2 Data Normalization

Data was normalized to enable more consistency in assessment of trends. The following provides an overview of process utilized to normalize the primary data inputs to the landslide model: displacement data and hydroclimatic data.

4.2.1 Displacement Data Normalization

As described by Froese et al (submitted), a displacement dataset obtained from over 500 slope inclinometers (SIs) from across the WCSB was compiled, screened and optimized to select datapoints meeting the following criteria:

- At least five years of monitoring data had been collected with a requirement that at least one significant acceleration event had been observed over that timeframe
- The instruments were read at least once per year and during appropriate times of the year such that annual displacements could be assigned to each landslide year (March to October)
- The observed displacement data were consistent with landslide displacement and not noise due to poor installation, or other error.

Based on the above screening stages (Froese et al, submitted) a high-quality dataset consisting of 641 annualized displacement data points was derived. At each instrument location, displacements measured along a landslide shear zone were normalized using a Minimum-Maximum approach (Uragan & Rajan, 2011). A value of 0 was assigned to the lowest observed annual displacement rate, a value of 1 was assigned to the highest observed annual displacement rate, and linear scaling was used to assign values between 0 and 1 to all other annual displacements that were recorded. The process of normalization allowed for trends in movement rates to be compared within instruments with multiple landslide shear surfaces and across instruments installed in landslides that typically moved at different annual rates. The distribution of the normalized values obtained from the 641 annualized displacements is shown in Figure 5.

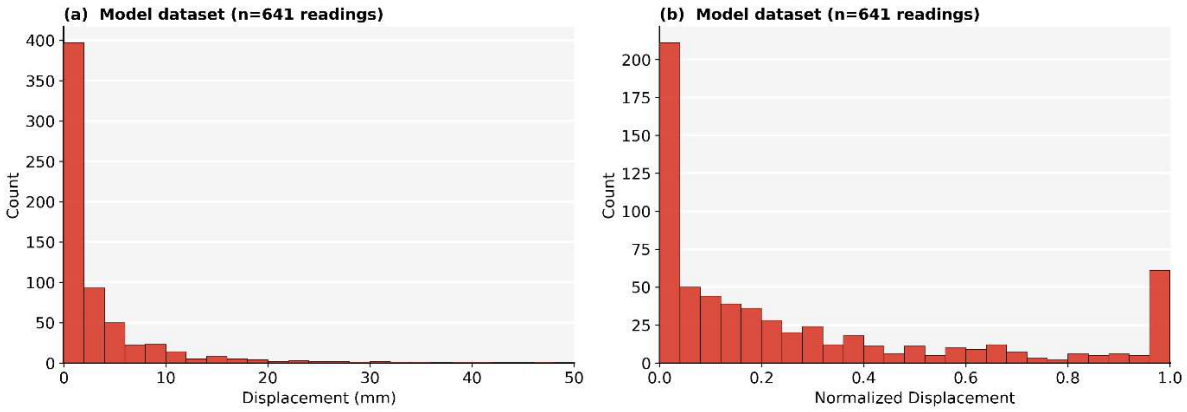


Figure 5. SI Data Distribution.

Based on a critical review of the distribution of the normalized displacement data the following rate categories were proposed:

- Slower than typical (<0.05) – typically involving annual displacements less than two millimetres per year, and landslides that were dormant during the landslide year
- Typical (0.05 to 0.2) – typically involving annual displacements between 1 and 4 millimetres per year
- Faster than typical (0.2 to 0.4) – typically involving annual displacements between 3 and 8 millimetres per year
- Much faster than typical (>0.4) – typically involving annual displacements greater than 8 millimetres per year, and often much greater

These values were utilized to support the development of the regional landslide forecast model. Much faster landslide displacements were recorded in several slope inclinometers, many of which occurred in 2020 or 2021, but the period of record for these instruments was often too short to be included in the statistical analysis or the instruments sheared off during this period preventing displacement measurements from being made.

4.3.3 Hydroclimatic Data Normalization

When considering the variability in soil moisture over time across the WCSB, the key indicator to understand in terms of landslide activity was the relative wetness and how best to represent this utilizing the ERA-5 dataset. To best understand the most appropriate normalization technique, sample time series data from representative location across the WSCB were assessed to understand the distribution of the data. Figure 6 provides samples of the six areas chosen for assessment.

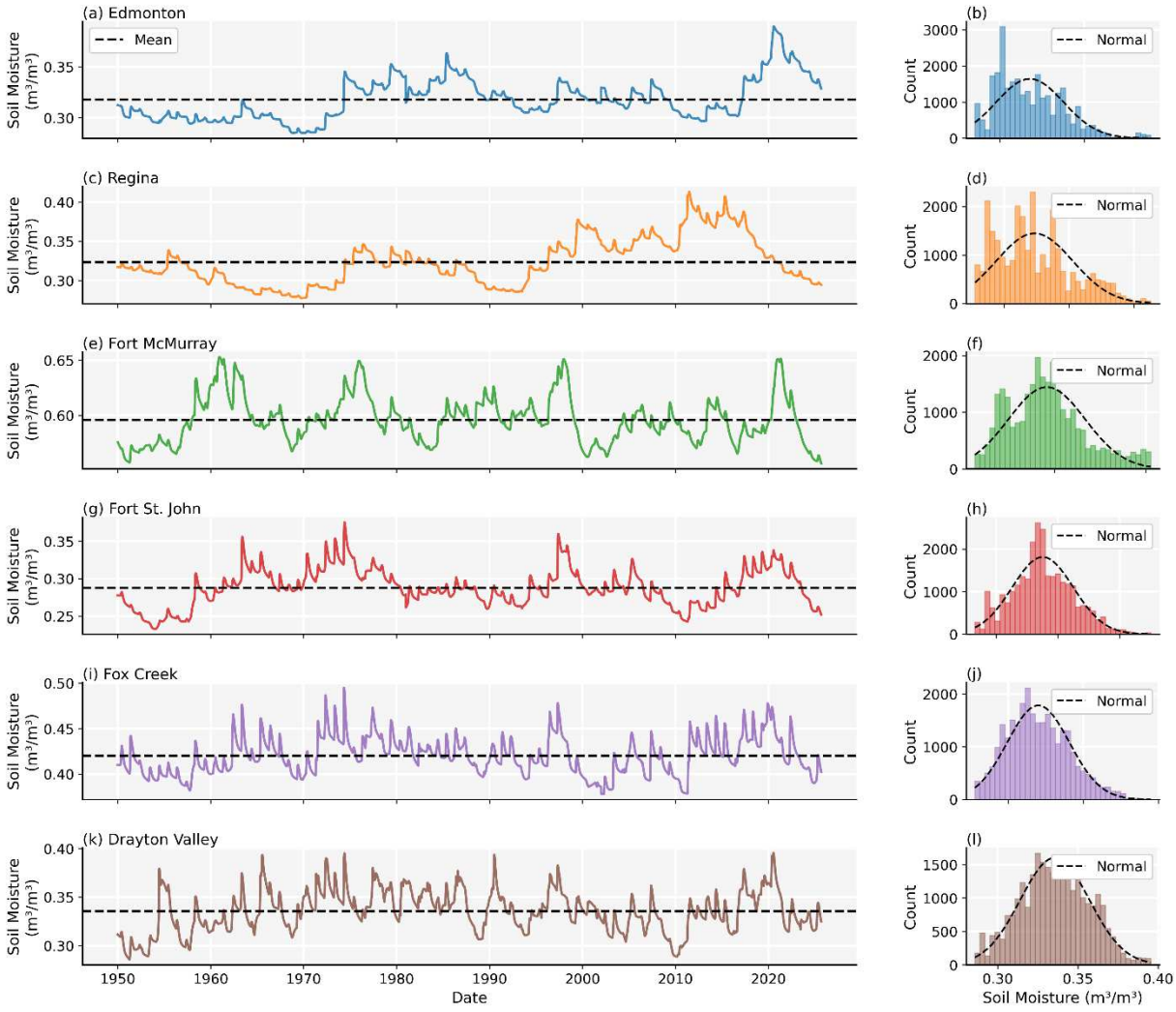


Figure 6. Timeseries of volumetric soil moisture values reported at selected locations across the study area (a, c, e, g, l, k; see Figure 2) and their distributions (b, d, f, h, j, l) for the period of 1950 to 2024.

As shown in Figure 6, normal distributions are not always evident. For example, the data associated with Edmonton or Regina present visual evidence of a skewed distribution. If data are normally distributed, the representation of a deviation from mean would not provide a meaningful method for illustrating extremes. To provide a more consistent method to normalize the soil moisture data across all regions, the concept of reporting on soil moisture values at each value as either minimum-maximum or percentile non-exceedance was proposed. While the percentile non-exceedance has the advantage of normalizing data in terms of the rarity of a value being realized, the Minimum-Maximum approach was chosen as the most appropriate technique to utilized to support the development of forecast models.

4.4 Understanding Importance of Key Hydroclimatic Drivers

The ERA-5 model derives and provides data for a total of 53 variables that described the water and energy cycles over the earth's land mass (Munoz-Sabater et al, 2021). To determine the most appropriate variables to consider with respect to landslide activity drivers it is important to consider the key contributors to water balance change both within and across landslide seasons was considered. As previously defined by Froese et al (In Preparation), the landslide season can be broken into the following seasonal phases:

- Freshet (March/April): following a long, cold winter, warmer temperatures lead to the melting of snowpack and the thawing of the ground, allowing infiltration into the subsurface. In the spring, sustained precipitation further adds to the infiltration leading to a relatively rapid rise in pore pressures at depth. This increase in pore pressures weakens the soil/rock in the subsurface and can lead to initiation of movements along existing shear zones.
- Late Spring/Early Summer (May/June): during this period the spring infiltration has "primed" landslides and they continue to accelerate. Average weekly precipitation levels often peak by late June. In parallel, as temperatures rise and vegetation establishes on the ground and on trees, the degree of evapotranspiration increases and this, coupled with reduced rainfall, begins to limit water infiltration past the tree root depth.
- Late Summer (July/August): the combination of warmer temperatures, well established vegetation and less precipitation leads to a significant reduction in moisture infiltration and landslides begin to slow.
- Autumn (September/October): typically, there is less precipitation at this time of the year and landslides move into a more normal or stable state and velocities are reduced.
- Winter (November to February): ground freezes and water infiltration is further reduced. Landslide movements either cease or are maintained at a low rate of displacement until freshet. With these seasons the following are the key groupings of parameters that were considered for the subsequent stages of modelling.

Based on these physical processes of both the longer and shorter duration trends described above, the following (Table 2) suite of ERA-5-derived parameters were considered for constructing a landslide movement model:

Table 2. ERA-5 derived parameters considered for model building.

Hydroclimatic Condition	Parameter	Parameter Description	Measurement Date/Period
Antecedent (Base) Soil Moisture	Base soil Moisture for Period Preceding Freshet (Normalized)	Average soil moisture (Layer 4) for the month of February, normalized, compared against all other February's in the record	February 1
	Multi-Year Rolling Wetness (Percentile)	Average annual soil moisture (Layer 4) expressed as a percentile against all other years in the record, averaged for X years prior to the landslide year	1, 2, 3, 4, 5 years
	Sustained Wetness	Maximum soil moisture (percentile) reported during the landslide season	Days prior to April 1
	Preceding Wetting (or Drying) Trend	Slope of wetting trend preceding the currently landslide year	1, 2, 3, 4, 5 years
Landslide Season Soil Moisture Inputs and Change	Maximum Value During Season (Percentile)	Maximum daily soil moisture (percentile) recorded for the landslide year	March to October
	Maximum Rate of Change During Season	Maximum slope of soil moisture trend (percent change/year) observed during different time durations throughout the landslide season.	7, 15, 30, 60, 90 days and Full Season (March to October)
Landslide Season Water Inputs	Precipitation Accumulations (mm and Normalized)	Accumulated daily precipitation over moving window of X days between March 1 and October 31.	1, 7, 13, 30, 60, 90 days
	Snowmelt Accumulation Maximums (mm and Normalized)	Accumulated daily snowmelt over moving window between March 1 and October 31	1, 7, 13, 30, 60, 90 days March to May
	Total Water Rolling Accumulation Maximums (mm and Normalized)	Accumulated daily total water over moving window between March 1 and October 31	1, 7, 13, 30, 60, 90 days March to May March to October

This screening yielded a set of 40 derivatives of the key variables which were then obtained corresponding to every displacement data point in the data cube to support trend analyses. Based on the results on previous experience and judgement of the senior landslide professionals on the project team, the following key parameters were chosen as the primary drivers for consideration in the landslide model:

- Normalized Soil Moisture at the beginning of the landslide season
- 1-year Normalized Soil Moisture trend at the beginning of the landslide season

- Total Water (Snowmelt and Precipitation) Rolling Accumulation during the landslide season.

These three variables were incorporated into the further stages of the model development.

5.0 Landslide and Warning Model Development

The focus of the landslide model development was to explore quantifiable linkages between activity levels of populations of landslides across the region in relation to the three primary hydroclimatic drivers. To support the operational implementation both the potential end-use and data granularity were considered in terms of what level of segmentation was possible with respect to states of landslide activity that could be supported by the data. These considerations are discussed in the following sections.

5.1 Defining the Regional Landslide Activity Index

Within areas experiencing similar hydroclimatic forcing, the expectation is that most landslides will move at typical or slower than typical rates under unusually dry conditions, and the majority will move faster or much faster than typical under unusually wet conditions. Because deep-seated landslide mechanisms are complex, and stability is controlled by other factors including toe erosion, forest fire activity, construction activities, and slope stabilization activities, some landslides will behave contrary to the expected trends. Based on this understanding, the objective of the landslide forecast model is to assign one of four Regional Landslide Activity Index (RLAI) categories to each landslide year that represent different probability distributions of landslides moving in the different normalized displacement rate categories. The different landslide year hindcast and forecast categories are described qualitatively in Table 2 and a quantitative representation is provided in Figure 7.

Table 3. Qualitative Description of Regional Landslide Activity Index categories.

Low Activity Year	Regional soil moisture and trends are below average. Most deep-seated landslides in the region are expected to be dormant or move more slowly than in typical landslide years. Most landslide movement rates are unlikely to increase beyond typical levels unless unusually large rainfall and/or snow melt occurs during the remainder of the landslide year. Exceptions may include landslides subject to toe erosion, forest fire, human disturbance, or progressive failure, which may continue to move faster than typical in spite of the drier conditions.
Typical Activity Year	Regional soil moisture and trends appear average. Many deep-seated landslides in the region are expected to be dormant or experience typical movement rates. Exceptions may include landslides subject to toe erosion, forest fire, human disturbance, or progressive failure, which may move faster than typical. Landslide activity and movement rates may increase beyond typical levels if above-average rainfall and/or snow melt occurs during the remainder of the landslide year.
High Activity Year	Regional soil moisture and trends are above average. Fewer than typical numbers of deep-seated landslides are expected to remain dormant, and many deep-seated landslides in the region are expected to experience above-typical movement rates. Landslides subject to toe erosion, forest fire, human disturbance, or progressive failure are expected to move faster than typical. Landslide activity and movement rates are likely to remain above typical levels unless below-average rainfall and/or snow melt occurs during the remainder of the landslide year.
Very High Activity Year	Regional soil moisture and trends are well-above average. Most deep-seated landslides in the region are likely to experience above-typical levels of activity and movement rates. Landslides subject to toe erosion, forest fire, human disturbance, or progressive failure are expected to move much faster than typical. Landslide activity and movement rates are likely to remain well-above typical levels even if below-average rainfall and/or snow melt occurs during the remainder of the landslide year.

These key index categories were chosen to define the zones for the warning model for which the assessment of the trends of the displacement and hydroclimatic data would be evaluated against.

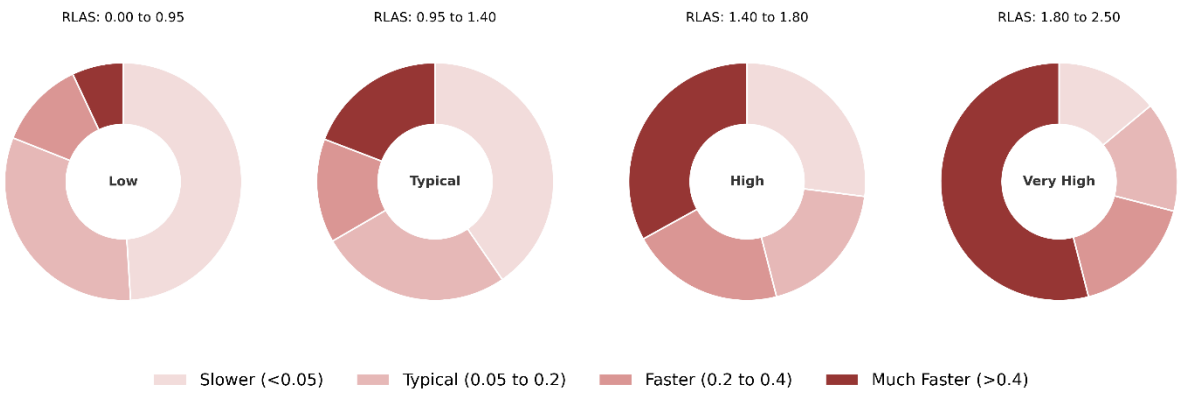


Figure 7. Distributions of landslide populations corresponding to calculated RLAS for historical normalized displacement data across the WCSB.

5.2 Determining Regional Landslide Activity Scores

As discussed in Section 4.4 the following key hydroclimatic variables, derived from the ERA-5 Land global gridded dataset, were defined as important predictors of landslide activity:

- Pre-Landslide Season Normalized Soil Moisture (NSM_{PLS}): the monthly average volumetric soil moisture in the deepest ERA-5 soil moisture model layer, observed around the month of February.
- Pre-Landslide Season Preceding 1-yr Soil Moisture Trend ($NSMT_{PLS1yr}$): the observed trend in deep soil moisture content over the preceding year (e.g. from February to February).
- Landslide Season 90-day Total Water Rolling Accumulation ($TWRA_{90}$): the maximum observed total water (snow melt and rainfall) added over a rolling 90-day window within the landslide season, which typically occurred during the months of May, June and July. The model is explained in Appendix A.

Like the treatment of the slope inclinometer data, each of the hydroclimatic variable values were normalized at each model grid cell. Values of 0 were assigned to the lowest parameter value observed over the approximately 75-year period of record, and values of 1 were assigned to the highest value observed. As a result, values between 0 and 1 could be assigned to every model grid cell for each parameter and for every landslide year.

Independent statistical evaluation of these three variables indicated that they were all important but that the preceding 1-yr soil moisture trend had lower predictive power than the other variables. Consequently, the normalized 1-yr soil moisture trend value was given half the weight of the other two parameters included in the predictive model, shown as follows:

$$RLAS = (1.0 \times NSM_{PLS}) + (0.5 \times NSMT_{PLS1yr}) + (1.0 \times TWRA_{90})$$

where: RLAS is the Regional Landslide Activity Score, ranging from 0 to 2.5. A combination of low normalized values would represent very dry conditions, represented by a low RLAS (theoretically as low as 0.0). Conversely, a very wet landslide season would yield a high RLAS (up to a maximum of 2.5).

Based on the above a RLAS value was derived for each of the 641 normalized annual displacements. Based on distributions of normalized landslide velocity groupings across the data, the binning of RLAS shown in Table 4 was proposed to generate the four RLAI categories.

Table 4. Regional Landslide Activity Index (Categories) chosen to represent activity of landslide populations in relation to the Regional Landslide Activity Scores (RLAS) obtained based on relations between historical landslide activity and hydroclimatic drivers.

RLAI Category	**RLAS Range**	**Interpretation**
Low Activity	RLAS < 0.95	Majority of landslides moving at typical or slower-than-typical rates (e.g., ~81% in the calibration data at or below typical).
Typical Activity	0.95–1.40	Mixed; many landslides dormant or typical, with a moderate share moving faster than typical.
High Activity	1.40–1.80	Majority moving faster or much faster than typical (e.g., ~71% in the calibration data).
Very High Activity	RLAS > 1.80	Most landslides likely to experience above-typical activity and movement rates.

The proportion of landslides moving at the different normalized rates for each RLAI category shown in Table 4 are the values that were used to generate the pie charts shown in Figure 7. For example, during a Low Activity Year (RLAS less than 0.95), the large majority of landslides (81%) in the slope inclinometer dataset moved at rates Typical or Slower than typical, while less than 20% of landslides moved at rates Faster or Much Faster than typical. Conversely, during a High Activity Year (RLAS between 1.40 and

1.80) the majority of landslides (71%) moved Faster or Much Faster than typical with a much smaller subset moving at or below Typical rates.

The expectation is that the statistical correlation between normalized displacement rate trends versus RLAS that were observed in the slope inclinometer data are likely also applicable at other locations across the WCSB where high-quality landslide displacement data are not yet available. Qualitative model validation was undertaken as an initial step in confirming this assumption, and additional validation will be undertaken in 2026.

5.3 Review of Model Hindcast Performance

In addition to the subset of slope inclinometer monitoring data there are a number of sites across the study area where both the monitoring data and experience from senior staff have been utilized to highlight key periods where elevated activity levels led to operational interventions. Anonymized Site IDs and key elevated activity periods are provided in Section 4.2.2, Table 1.

For each location, the landslide model prototype was run across a time period leading up to and encompassing these elevated activity periods to examine the following:

- Pre-Season RLAI forecasts based on the 95th Percentile, Mean and 5th Percentile in relation to the 75-year hydroclimate data record.
- RLAI at the end of each month during the landslide season (95th Percentile, Mean and 5th Percentile)
- End of Season RLAI derived from the actual maximum 90-day total water rolling accumulation during the landslide season.

As an example, Figure 8, provides the Pre-Season RLAI forecast for Site G, while Figure 9 provides the actual RLAI realized at the end of the landslide season at that site.

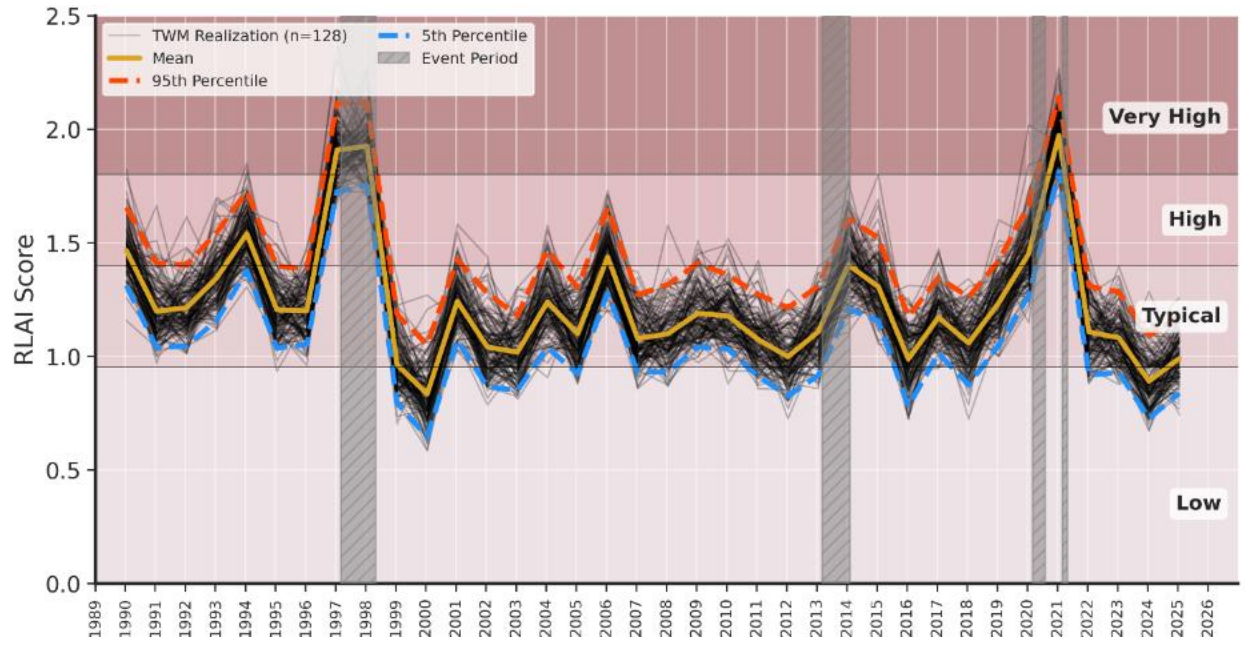


Figure 8 Pre-Season RLAI score forecasts (made at the end of February) for Site G from 1989 to the end of 2025.

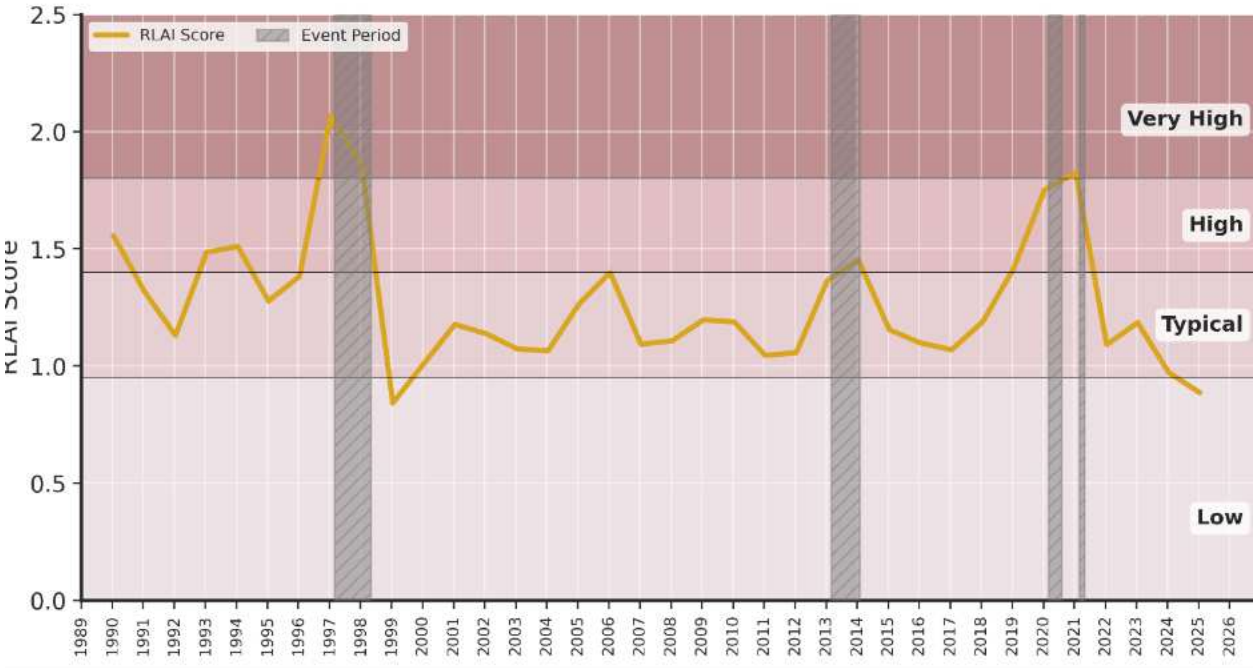


Figure 9 End of season actual RLAI scores for Site G from 1989 to the end of 2025.

In reviewing the above figures, the key observations in terms of the quality of the forecasts derived from the pre- and post-landslide season RLAI are as follows:

- 1997 – 1998: The 1996 pre-season forecast indicated that the 95th percentile would advance the site to a High Activity condition, and by 1997 both the pre-season 95th percentile and Mean values forecast a Very High Activity season. Both of these forecasts preceded the initiation of elevated activity levels.
- 2005 – 2006: Both the 95th percentile and Mean pre-season forecasts for the 2006 landslide season indicated the potential to transition into a High Activity season. When reviewing the actual RLAI scores achieved, they did not yield values that transitioned into the High Activity condition, likely indicating that the modelled total water accumulations that season were less than the historical mean. Landslide activity during this period did not trigger a significant operational response.
- 2013 – 2014: Prior to the 2013 landslide season, the 95th percentile prediction was at the high end of Typical Activity Season and the mean value plotted within a Typical range. The actual values plotted in the low end of the High Activity zone, indicating that total water accumulations during the landslide season were greater than the 95th percentile.
- 2020 – 2022: Prior to the 2020 landslide season, both the 95th percentile and mean forecast values were in the High to Very High Activity range, indicating that a large proportion of landslides in the region were likely to be moving at rates much faster than typical.

Similar model performance was observed at the other key sites. There were a few instances where the early forecast RLAI would have generated a false positive, and very few instances where the early forecast RLAI would have generated false negatives. In nearly all cases, the end-of-season RLAI align well with observed landslide activity that triggered an operational response. It is important to state that the intent of the RLAI is to provide awareness to support preparedness, not to provide a definitive alert level to be associated with site specific response. This being said it is expected that an asset owner would have sufficient awareness of the risks and conditions of their system in order to utilize the RLAI trends to support proactive review and management.

5.4 Initial 2026 Forecasts

The relationships used to develop hindcasts were utilized to develop and deliver the first annual landslide forecast for the 2026 season was issued in March 2026.

The forecast uses normalized soil moisture and trend values from February 1, 2026, alongside a probabilistic prediction of the maximum 90-day total water accumulation during the season. This accumulation is a strong predictor of landslide activity but is not known in advance. To estimate it, a statistical model fitted to approximately 75 years of ERA5-Land data generates Monte Carlo simulations of daily total water at each grid cell, producing a probability distribution of RLAS and RLAI. This enables probabilistic forecasts represented as 5th, 50th, and 95th percentile (Figure 10) maps that capture both the most likely outcome and the range of plausible extremes.

Uncertainty narrows progressively as the landslide season advances. Early in the season, the 90-day accumulation is almost entirely simulated, so the spread between percentile forecasts is at its widest. Each month, observed data replaces simulated values in the rolling accumulation until, by season's end, the three maps converge to a single deterministic RLAI classification. Monthly bulletins will be issued through September, after which final RLAI values will be published in the fall to inform operational planning for the following year.

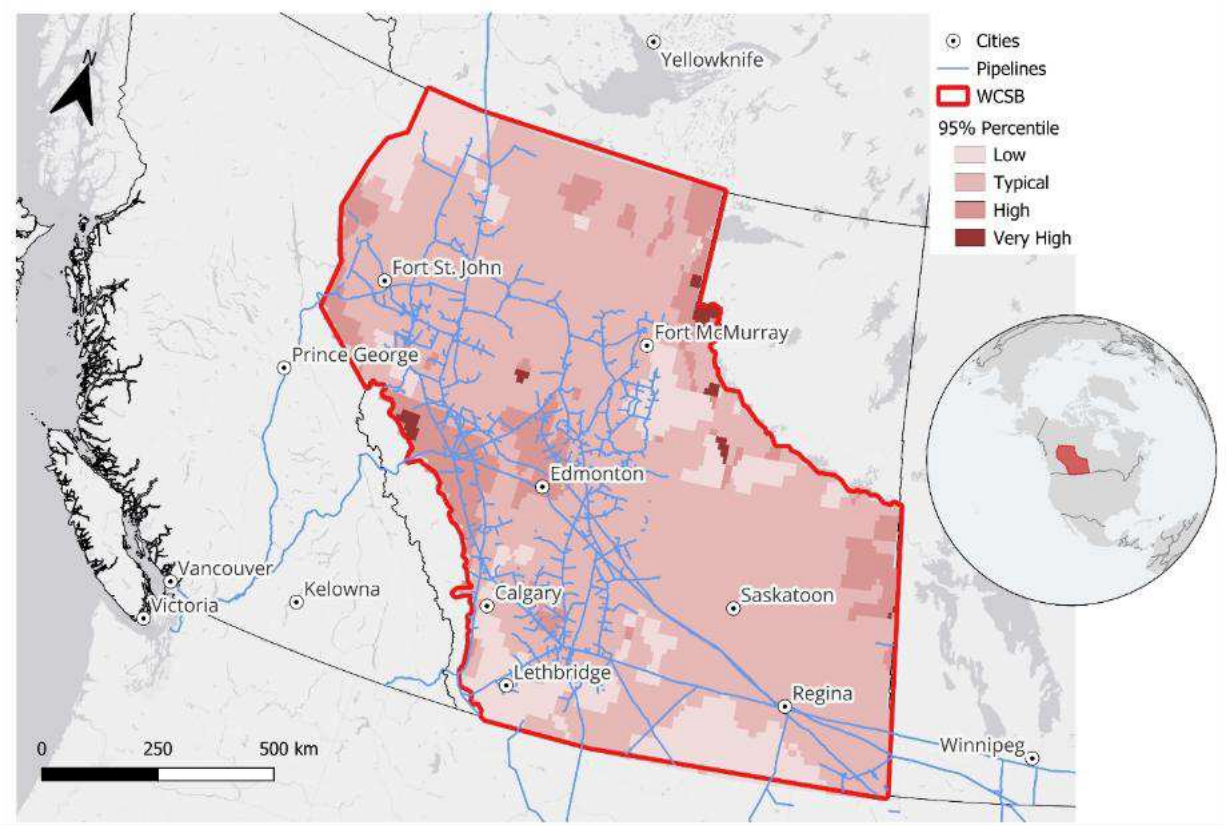


Figure 10. 95th percentile predictions for RLAI in March 2026. Data sources: ESRI tiles, Natural Earth and HIFLD Canadian pipeline dataset, BGC Engineering.

6.0 Next Steps for Implementation and Model Improvement

The initial RLAI categorization in terms of both the activity normalization and the relative weighting to the hydroclimatic drivers has been developed based on the available historic manually-read displacement data across the region. It is expected that the modelled relationships will continue to improve and potentially allow for more granularity in both spatial and temporal prediction with the addition of data that will become more widely available across the region. Some of the key improvements planned for consideration are as follows.

Networked Arrays of Continuously Monitored Landslides

At the time of the writing of this paper, there are well over 100 shape accelerometer array (SAA) installations within the WCSB that are owned/operated by the project contributors that obtain data every one to six hours at landslide locations. As the data from these installations is telemetered and centrally managed there is an opportunity to continue to grow the displacement dataset utilized to calibrate the RLAI model.

L-Band InSAR Data

With the launch of the NASA and Indian Space Research Organization (ISRO) NISAR satellite in the summer of 2025, there are stacks of L-Band Synthetic Aperture Radar (SAR) data being collected over the WCSB. NASA has indicated that scientific quality data collection began in the fall of 2025 and that data would begin to become publicly available in summer 2026. It is expected that additional landslides in the WCSB with favorable geometries will be added to the sites tracked in the region and the data added to the dataset. Although the line of sight (LOS) data from the SAR satellite only provides a component of the displacement the similar normalization technique will be utilized to support relative understanding as to the magnitude of annual displacements.

Finer Resolution Hydroclimatic Data and Models

With the ever-increasing data available from satellites and telemetered ground sensors, the ability to track and model conditions on the earth and in the atmosphere will continue to advance. By coupling higher frequency and resolution displacement data with these hydroclimatic data there are opportunities to better understand the relative contribution of different hydroclimatic drivers in the initiation of landslide displacements at a finer temporal and spatial resolution.

7.0 Conclusions

Slowly moving DSLs in the Western Canadian Sedimentary Basin lead to ongoing strain and damage to infrastructure than drive significant financial investments by asset owners. As asset owners determine appropriate actions based on the condition of the infrastructure and the ability to accommodate strain, they require an understanding as to how trends develop over both space and time to support proactive management. This study has integrated over 30 years of displacement data for DSLs and explored the correlations with modelled hydroclimatic data over the same time period to better understand the key drivers for landslide activity changes across the region. These relations have been utilized to develop a Regional Landslide Activity Index (RLAI) to inform asset owners as to how populations of landslides would be expected to perform in relation to a key suite of hydroclimatic drivers. A set of Regional Landslide Activity Scores (RLAS) have been calibrated based on how they best represent the landslide performance represented in the RLAI and have been validated against known sites to assess how they can support operational decision making.

8.0 Acknowledgements

This work has been generously supported in terms of funding, data and feedback by the following organizations: Enbridge Liquids, TC Energy, Pembina Pipeline, Inter Pipeline, SaskEnergy, Fortis BC, BC Hydro and Alberta Transportation and Economic Corridors.

The technical delivery for this project has been supported by the following colleagues: Evelyn Moorehouse, Mark Halverson, Pat Grover, Arnaud Michel, David Gauthier, Richard Carter, Peter Barlow, Joel Van Hove, Zac Sala

9.0 Competing Interests

The authors disclose that there are neither financial nor non-financial interests that directly or are indirectly related to the work submitted for publication.

10.0 Funding

The authors acknowledge support in terms of financial contributions and data from the following organizations: Enbridge, TC Energy, Pembina Pipelines, Inter Pipeline, Sask Energy, Fortis Energy, Alberta Transportation and Economic Corridors, BC Hydro.

11.0 Data Availability Statement

The datasets generated during and/or analysed during the current study are not publicly available due as they were derived under contractual agreements with private corporations. That being said, these data may be made are available from the corresponding author on reasonable request.

12.0 Consent to Publish Declaration

Not Applicable

13.0 Ethics and Consent to Participate Declaration

None of the data derived for this study were obtained from tests utilizing humans or animals. Therefore neither consent to participate nor any ethical declarations are applicable to this submission.

14.0 Clinical Trial Number

Not Applicable

15.0 References

Ahmadipur, A., McKenzie-Johnson, A., Ebrahimi, A., & Rice, A. H. (2020, September). Identification and Mitigation of a Landslide Threatening Four Operating Natural Gas

Pipelines. In International Pipeline Conference (Vol. 84461, p. V003T04A025). American Society of Mechanical Engineers.

Alaminie, A. A., Annys, S., Nyssen, J., Jury, M. R., Amarnath, G., Mekonnen, M. A., & Tilahun, S. A. (2024). A comprehensive evaluation of satellite-based and reanalysis soil moisture products over the upper Blue Nile Basin, Ethiopia. Science of Remote Sensing, 10, 100173.

BGC Engineering. 2020. Northeast British Columbia Landslide Susceptibility Map. Report for the BC Oil and Gas Research and Innovation Society submitted December 17, 2020. BGC Report 2178001. https://www.bc-er.ca/files/gis/2178001-BC_OGRIS_NE_BC_Landslide_Susceptibility.pdf Calvello, M. (2017). Early warning strategies to cope with landslide risk. Rivista italiana di geotecnica, 2(17), 63-91.

Chen, H., Li, G., Fang, R., & Zheng, M. (2021). Early warning indicators of landslides based on deep displacements: applications on Jinping landslide and Wendong landslide, China. Frontiers in Earth Science, 9, 747379.

Coe, J. A. (2012). Regional moisture balance control of landslide motion: Implications for landslide forecasting in a changing climate. Geology, 40(4), 323-326.

Conte, E., Donato, A., & Troncone, A. (2014). A finite element approach for the analysis of active slow-moving landslides. Landslides, 11(4), 723-731.

Dewar, D., Tong, A., McClarty, E., & Van Boven, G. (2016, September). Technical and operational guidelines when using strain gauges to monitor pipelines in slow moving landslides. In International Pipeline Conference (Vol. 50275, p. V003T04A023). American Society of Mechanical Engineers.

Distefano, P., Peres, D. J., Piciullo, L., Palazzolo, N., Scandura, P., & Cancelliere, A. (2023). Hydro-meteorological landslide triggering thresholds based on artificial neural networks using observed precipitation and ERA5-Land soil moisture. Landslides, 20(12), 2725-2739.

Dowling, C. A., Quinn, P., Lloyd, M., Dipple, M., & McPherson, R. (2019, September-October). Landslide susceptibility mapping for large landslides in Saskatchewan. GeoStJohn's 2019: Under land and sea. Paper presented at the meeting of the Canadian Geotechnical Society, St. John's, NL.

European Centre for Medium-Range Weather Forecasts, (2016). Part IV: Physical Process. IFS Documentation – Cy31r2, Operational implementation 8 March 2016. Published by the European Centre for Medium-Range Weather Forecasts.
DOI: https://doi.org/10.21957/tr5rv27xu

Finnegan, N. J., Perkins, J. P., Nereson, A. L., & Handwerger, A. L. (2021). Unsaturated flow processes and the onset of seasonal deformation in slow-moving landslides. Journal of Geophysical Research: Earth Surface, 126(5), e2020JF005758.

Froese, C., Porter, M., Stringari, C., Coia, V. Submitted. Integrating displacement data for slowly moving landslides to support regional landslide model development.

Guzzetti, F., Gariano, S. L., Peruccacci, S., Brunetti, M. T., Marchesini, I., Rossi, M., & Melillo, M. (2020). Geographical landslide early warning systems. Earth-Science Reviews, 200, 102973.

Handwerger, A. L., Roering, J. J., & Schmidt, D. A. (2013). Controls on the seasonal deformation of slow-moving landslides. Earth and Planetary Science Letters, 377, 239-247.

Khan S, Kirschbaum DB, Stanley TA, Amatya PM and Emberson RA (2022) Global Landslide Forecasting System for Hazard Assessment and Situational Awareness. Front. Earth Sci. 10:878996. doi: 10.3389/feart.2022.878996

Lacroix, P., Handwerger, A. L., & Bièvre, G. (2020). Life and death of slow-moving landslides. Nature Reviews Earth & Environment, 1(8), 404-419.

Li, P., He, L., Wang, X., Ding, E., & Yu, Q. (2025). How reliable are long time-series reanalysis and model-based soil moisture products for agricultural soil water stress monitoring? Insights from a five-dataset evaluation across China. Agricultural Water Management, 320, 109845.

Mansour, M. F., Morgenstern, N. R., & Martin, C. D. (2011). Expected damage from displacement of slow-moving slides. Landslides, 8(1), 117-131.

Mazziotta, M., & Pareto, A. (2022). Normalization methods for spatio-temporal analysis of environmental performance: Revisiting the Min–Max method. Environmetrics, 33(5), e2730.

Mirus, B. B., Bogaard, T., Greco, R., & Stähli, M. (2025). Invited perspectives: Integrating hydrologic information into the next generation of landslide early warning systems. Natural Hazards and Earth System Sciences, 25(1), 169-182.

Mirus, B. B., Morphew, M. D., & Smith, J. B. (2018). Developing hydro-meteorological thresholds for shallow landslide initiation and early warning. Water, 10(9), 1274.

Muñoz Sabater, J., Dutra, E., Agustí-Panareda, A., Albergel, C., Arduini, G., Balsamo, G., Boussetta, S., Choulga, M., Harrigan, S., Hersbach, H. and Martens, B., (2021). ERA5-

Land: A state-of-the-art global reanalysis dataset for land applications. Earth system science data, 13(9), pp.4349-4383.

Palazzolo, N., Cancelliere, A., Zofei, R. D., & Peres, D. J. (2025). Use of delayed ERA5-Land soil moisture products for improving landslide early warning. Natural Hazards and Earth System Sciences, 25(12), 4907-4919.

Pawley, S.M., Hartman, G.M.D. and Chao, D.K. (2017): Examples of landslides and the geological, topographic, and climatic factors that contribute to landslide susceptibilities in Alberta - a cross-reference to the explanatory notes for AGS Map 605; Alberta Energy Regulator, AER/AGS Information Series 148, 26 p.

Porter, M., Van Hove, J., Barlow, P., Froese, C., Bunce, C., Skirrow, R.,& Bobrowsky, P. (2019, September). The estimated economic impacts of prairie landslides in western Canada. In Proceedings of the 72nd Canadian Geotechnical Conference, St. John's, NL, Canada (Vol. 29).

Porter, M., Van Hove, J., Bunce, O., & Barlow, P. (2023, November). Risk Assessment and Cost Benefit Analysis for Pipelines Buried in Slow-Moving Landslides.
In International Pipeline Geotechnical Conference.

Rana, D., Dadkhah, H., Ghaderpour, E., Bozzano, F., & Mazzanti, P. (2026). Monitoring slow-moving landslides through PS-InSAR and antecedent precipitation index: a case study of Petacciato, Italy. International Journal of Remote Sensing, 1-30.

Sättele, M., Bründl, M., & Straub, D. (2016). Quantifying the effectiveness of early warning systems for natural hazards. *Natural Hazards and Earth System Sciences*, *16*(1), 149-166.

Segoni, S., Rosi, A., Fanti, R., Gallucci, A., Monni, A., & Casagli, N. (2018). A regional-scale landslide warning system based on 20 years of operational experience. Water, 10(10), 1297.

Sengani, F., & Mulenga, F. (2022). A review on the application of particle finite element methods (PFEM) to cases of landslides. International Journal of Geotechnical Engineering, 16(3), 367-381.

Uragun, B., & Rajan, R. (2011, December). Developing an appropriate data normalization method. In 2011 10th international conference on machine learning and applications and workshops (Vol. 2, pp. 195-199). IEEE.

Wicki, A., Jansson, P. E., Lehmann, P., Hauck, C., & Stähli, M. (2021). Simulated or measured soil moisture: which one is adding more value to regional landslide early warning?. Hydrology and Earth System Sciences, 25(8), 4585-4610.

Zandler, H., Senftl, T. & Vanselow, K.A. Reanalysis datasets outperform other gridded climate products in vegetation change analysis in peripheral conservation areas of Central Asia. Sci Rep 10, 22446 (2020). https://doi.org/10.1038/s41598-020-79480-y

Zieher, T., Gallotti, G., Rianna, G., Reder, A., & Pfeiffer, J. (2023). Exploring the effects of climate change on the water balance of a continuously moving deep-seated landslide. Natural Hazards, 115(1), 357-387.

Appendix A – Total Water Model

As previously mentioned, $TWRA_{90}$ is not available for generating forecasts. But more information about this quantity becomes available as the water year progresses. Therefore, a statistical model based on past probability distributions was developed to make use of the known information operationally. A Monte Carlo ensemble of plausible year-completions is generated from the model, the maximum 90-day rolling accumulation is computed from each ensemble member, and the resulting distribution of $TWRA_{90}$ is propagated through the RLAS calculation. Consequently, the distribution of RLAS is wide at the start of the landslide year, reflecting the uncertainty in future precipitation and snowmelt, and tightens as additional observations accumulate.

Each ERA-5 grid cell within the WCSB has an associated daily total water time series, defined as the sum of daily total precipitation and daily snowmelt. W_t denotes the total water on day-of-year t for a given grid cell. For a window of k consecutive days, the k-day rolling accumulation S_t is computed as the sum of total water over day t and the preceding $k-1$ days,

$$S_t = \sum_{i=1}^{k} W_{t+1-i}, \quad t \in T,$$

where T denotes the set of days comprising the landslide year. The annual maximum k-day total water is

$$M = \max_{t \in T} S_t.$$

For the purposes of the RLAS, $k = 90$ days and the landslide year is defined consistent with the seasonal phases described before. Prior to use in the RLAS, M is normalized at the grid-cell level using the same minimum-maximum technique applied to the other hydroclimatic variables based on normalization constants determined from prior years' data.

The objective here is to describe how to obtain the distribution of the annual maximum M given the partially observed series up to the current day, denoted $\{W_t : t \leq today\}$. The development proceeds in two stages: model building and model sampling.

Model Building

To model the distribution of the total water time series across a landslide year ($W_t : t \in \mathrm{T}$), we use a simple Markovian model that models lag-1 serial dependence. More sophisticated models exist and should be considered for future iterations of the model (e.g., Papalexiou, 2018; see also the R package CoSMoS Strnad et al., 2021). First, we

estimate the marginal distribution of total water for each day of year using the empirical cumulative distribution function (CDF). For a sample of total water observed across multiple years for a particular day of year t, the empirical CDF is

$$F_t(x) = \frac{1}{N} \sum_{y \in Y} I\left(W_{t,y} \leq x\right),$$

where $W_{t,y}$ is the same total water W_t variable but also indexed by year, $N = |Y|$ is the number of years in the record, and I is the indicator function (1 if the condition is true, 0 otherwise). The empirical distribution was preferred over parametric families (e.g. lognormal, gamma) because it reproduces the non-standard shapes typical of daily total water without imposing a parametric form that may not apply uniformly across the WCSB.

We model lag-1 serial dependence with a bivariate Gaussian copula. We assume the dependence structure is time-invariant throughout the year and therefore pool data across days. A copula is a joint distribution with $Uniform(0, 1)$ univariate margins. It enables flexible multivariate modelling by separately specifying the marginal distributions for each day-of-year, and the dependence between them after transforming to uniforms via the probability integral transform:

$$U_t = F_t(W_t),$$

where $U_t \sim Uniform(0, 1)$ when F_t is the true CDF of W_t. The Gaussian copula is then adopted for each adjacent pair (U_t, U_{t-1}), with a single correlation parameter ρ.

Parameter Estimation

The copula correlation ρ (Figure 7) is estimated from the Pearson correlation of normal scores on consecutive days. For each observation, the normal score is obtained by applying the corresponding day-of-year empirical CDF followed by the standard normal inverse,

$$Z_t = \Phi^{-1}\left(F_t(W_t)\right),$$

where Φ^{-1} denotes the standard normal quantile function. Consecutive-day pairs (Z_{t-1}, Z_t) are assembled within each calendar year, pooled across years, and ρ is taken as the sample Pearson correlation of the pooled pairs.

Once fitted, the entire distribution of the total water time series W_t at each grid cell is fully specified by: (i) the day-of-year empirical CDF F_t (and its corresponding quantile function) for every day of the year; and (ii) a single Gaussian copula correlation parameter ρ. No

closed-form multivariate CDF for the full time series is required, because the joint distribution is used only for simulation.

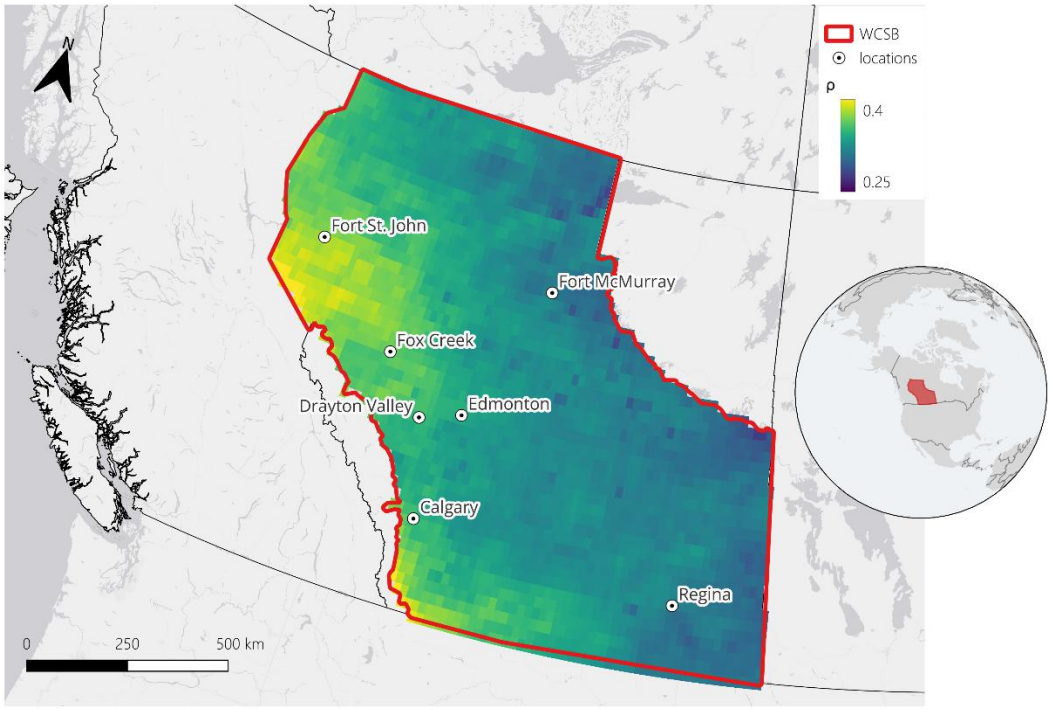


Figure 7. Fitted parameter ρ, the level of serial dependence between subsequent days' total water.

Model Sampling

Given the partially observed series $\{W_t : t \leq today\}$, the remainder of the year is generated by exploiting the Markov property of the model: only the most recent observed value is required to step the simulation forward one day. Suppose that W_t has been observed on day t. The conditional quantile function of W_{t+1} given W_t is:

$$Q_{t+1\,|\,t}(\tau) \;=\; Q_{t+1}\left(C_{2|1}^{-1}\big(\tau \mid F_t(W_t)\big)\right), \quad \tau \in (0,1),$$

where $Q_{t+1} = F_{t+1}^{-1}$ is the marginal quantile function on day $t+1$ (i.e., the left-inverse of the CDF F_{t+1}) and $C_{2|1}^{-1}$ is the inverse of the conditional copula CDF:

$$C_{2|1}(v|u) = \frac{\partial}{\partial u} C(u,v),$$

where C is the copula CDF. For the Gaussian copula with correlation ρ , the conditional sampling used in the numerical implementation reduces to the standard form

$$Z_{t+1} \mid Z_t \;\sim\; N(\rho\, Z_t, 1 - \rho^2),$$

A single Monte Carlo draw proceeds as follows:

1. Compute the uniform score of the last observed value, $U_t = F_t(W_t)$, and the corresponding normal score $Z_t = \Phi^{-1}(U_t)$.
2. Draw Z_{t+1} from the conditional Gaussian $N(\rho\, Z_t, 1 - \rho^2)$ and map back first to the uniform scale as $U_{t+1} = \Phi(Z_{t+1})$ and then to the daily scale $W_{t+1} = Q_{t+1}(U_{t+1})$.
3. Advance the time index from t to $t + 1$, treat the newly generated value as the most recent observation, and repeat Steps 1–2 until the end of the landslide year is reached.
4. Compute the 90-day rolling accumulation S_t from the completed series (observed values followed by simulated values) and record the annual maximum M.
5. Repeat Steps 1–4 for the desired number of Monte Carlo iterations (500 in this case). The resulting ensemble of M values approximates the conditional distribution of the annual 90-day maximum total water given the observations available to date.

Early in the landslide year, few daily values are observed, and the ensemble distribution of M is wide, reflecting large uncertainty in the remainder of the year. As the season progresses, the distribution tightens and, by the end of the year, converges to the deterministic value implied by the fully observed series.

Regional Implementation

The total water model is fitted and applied independently at each ERA-5 grid cell within the WCSB. For each grid cell, the daily total water series is assembled from the full ERA-5 Land record, a grid-cell-specific set of day-of-year empirical marginals F_t is estimated, and a single grid-cell-specific lag-1 Gaussian copula correlation ρ is fitted from the pooled normal-score pairs of consecutive days. Grid cells that are entirely masked or that contain fewer than a minimum number of valid daily observations are flagged and excluded from prediction.

During prediction, the fitted grid-cell models are applied in parallel across the regional spatial domain. For a given target year and target day, the observed total water series up to the target day is passed to the sampler together with the fitted model, yielding an ensemble of simulated year-completions at each grid cell. The 90-day rolling accumulation is computed for each ensemble member, the annual maximum M is extracted, and the resulting distribution is min–max scaled against the grid-cell historical range and supplied to the RLAS calculation as $TWRA_{90}$.

References

Papalexiou, Simon Michael. 2018. “Unified Theory for Stochastic Modelling of Hydroclimatic Processes: Preserving Marginal Distributions, Correlation Structures, and Intermittency.” Advances in Water Resources 115: 234–52. https://doi.org/10.1016/j.advwatres.2018.02.013.

Strnad, Filip, Francesco Serinaldi, Simon Michael Papalexiou, Yannis Markonis, and Kevin Shook. 2021. CoSMoS: Complete Stochastic Modelling Solution. https://CRAN.R-project.org/package=CoSMoS.